Probing the Anisotropic Environment of Thermotropic Liquid Crystals Using ^{129}Xe NMR Spectroscopy

B. Jagadeesh,*,† A. Prabhakar,† M. H. V. Ramana Rao,† C. V. S. Murty,‡ V. G. K. M. Pisipati,§ A. C. Kunwar,† and C. R. Bowers‖

NMR Center and Chemical Engineering Division, Indian Institute of Chemical Technology, Uppal Road, Hyderabad 500 007, India; Department of Physics, Nagarjuna University, Nagarjuna Nagar, India; and Chemistry Department, University of Florida, Gainesville, Florida 32611

Received: December 8, 2003; In Final Form: May 12, 2004

The thermotropic liquid crystal (LC), 4,4′-diheptylazoybenzene (HAB), exhibiting isotropic nematic and smectic phases, is investigated through ^{129}Xe NMR and density studies. The temperature dependence of ^{129}Xe chemical shifts and spin−lattice relaxation times (T_1) of the xenon gas dissolved in HAB have shown clear signatures of the phase transitions. We have applied an extended pairwise additive model to the smectic phase of HAB to account for the measured temperature dependence of chemical shifts. It is inferred that the LC−xenon molecular pair correlations have a significant effect on the shielding anisotropy in the nematic and smectic phases whereas they are negligible in the isotropic phase. The isotropic and anisotropic parts of the nuclear shielding and their dependences on liquid crystalline ordering (orientational and translational), density, and temperature are deduced for both the nematic and smectic phases. It is found that the shielding anisotropy is primarily due to orientational ordering of the LC molecules. In the smectic phase, xenon atoms preferentially occupy interlayer spacings rather than their interiors, leading to an increase in the isotropic part of the shielding. The activation energies (E_a) associated with xenon dynamics in different phases are deduced from T_1 measurements. Despite the denser packing of molecules in the smectic phase, the E_a in this phase is lower than that of the nematic phase. This finding is in agreement with the conclusions drawn from the analysis of the chemical shift data.

Introduction

In recent years, NMR spectroscopy of xenon (^{129}Xe spin $^1/_2$ and ^{131}Xe spin $^3/_2$) gas has gained importance due to its sensitivity in probing environments of various materials, biological molecules, and organic solvents.[1−8] Xenon has a van der Waals diameter of 4.4 Å[5] and exhibits a wide range of chemical shift (∼300 ppm) values in the dissolved or physiadsorbed phases. While ^{129}Xe NMR spectroscopy has been widely used to study porous solids and liquids, relatively few studies have been devoted to understanding the ^{129}Xe nuclear shielding behavior in anisotropic fluids such as liquid crystals.

The focus of this paper is on the application of ^{129}Xe NMR to the study of liquid crystals (LCs). The remarkable properties of liquid crystals stem from the anisotropy associated with orientational order. Some nematic LCs are employed as solvents to orient guest molecules for NMR structural elucidation based on residual dipolar couplings.[9] In the smectic liquid crystalline phase molecules are arranged in layers, which leads to a one-dimensional density wave along the layer axis.[10] Molecular motion along the layer direction is restricted, and it is liquidlike in the planes perpendicular to this direction.

In free xenon gas the Xe atoms possess a spherical electron distribution; hence, they exhibit only the isotropic part of the chemical shift. However, in the liquid crystalline environment, the anisotropic forces cause partial orientation of the solute xenon atoms. This situation leads to a deformation of their spherical symmetry, which results in ^{129}Xe shielding anisotropy. The temperature dependence of ^{129}Xe chemical shifts carries information about the average molecular ordering and shielding anisotropy that can be analyzed in the framework of the mean-field approximation. Unlike ^{2}H NMR spectroscopy,[11] ^{129}Xe NMR of dissolved xenon gas does not require the painstaking isotopic labeling. Xenon-129 chemical shifts in some pure and binary mixtures of liquid crystals were reported earlier.[2,12−15] We have also studied the reentrant nematic phenomenon in LC mixtures using ^{129}Xe chemical shifts and spin-relaxation times.[14] However, due to the absence of a suitable theoretical model, the majority of these results were explained only qualitatively.

A phenomenological theory was developed by Lounila et al.[16] to account for the ^{129}Xe shielding behavior in isotropic, nematic, and smectic phases and was applied to a LC, NCB-84, that exhibits these three phases. According to this model, the temperature dependence of the ^{129}Xe chemical shift was attributed solely to the variation of the LC density and orientational order parameter, which has some limitations in explaining the temperature dependence of ^{129}Xe shielding satisfactorily.[17] Nevertheless, this phenomenological model offers basic theoretical arguments that are useful for analyzing the ^{129}Xe shielding behavior in LC phases.

Recently, Ylihautala et al. have developed a "pairwise additive" model[17,18] which could explain the temperature dependence of ^{129}Xe shielding in the nematic phase more satisfactorily. In the pairwise additive model, the contribution due to xenon−LC pair correlations is included and the temperature dependence

† NMR Center, Indian Institute of Chemical Technology.
‡ Chemical Engineering Division, Indian Institute of Chemical Technology.
§ Nagarjuna University.
‖ University of Florida.

10.1021/jp037745m CCC: $27.50
Published on Web 07/03/2004

of isotropic and anisotropic shielding constants is accounted for. However, so far this model has been applied to nematic LCs only.[17,18] Extending this model to the smectic phases would be interesting, as the smectic LCs serve as a model for a lipid bilayer, which is a major constituent of a living cell. For example, the lipid bilayer regulates the flow of O_2 and CO_2 gases and small polar molecules across the membrane.

In the present study, relying upon both of the earlier models, we have extended the pairwise additive model to the smectic phase and applied it to a LC, 4,4′-diheptylazoxybenzene (HAB), which exhibits phase transitions in the following sequence,[19]

$$\text{crystal} \xleftarrow[T_{CS}]{307\ \text{K}} \text{smectic-A} \xleftarrow[T_{SN}]{327\ \text{K}} \text{nematic} \xleftarrow[T_{NI}]{342\ \text{K}} \text{isotropic}$$

where T_{NI}, T_{SN}, and T_{CS} are the isotropic to nematic (I−N), nematic to smectic (N−S), and smectic to crystal (S−C) transition temperatures, respectively. The ^{129}Xe chemical shifts in HAB were previously reported by Jokisaari et al. but were analyzed only qualitatively.[13] However, in the present detailed investigations, the density of HAB and the ^{129}Xe chemical shifts of xenon gas dissolved in HAB are measured as a function of temperature and are quantitatively modeled to evaluate the isotropic deformation and anisotropic shielding contributions to the chemical shifts. Furthermore, we show how these properties are influenced by phase transitions. Information about the Xe dynamics and the hindering barriers is obtained from T_1 measurements. These results are corroborated with chemical shielding data.

Experimental Section

HAB (98%) was obtained from Sigma-Aldrich Corporation, Secunderabad, India, and used without further purification. Xenon gas (99.999%) was obtained from Hydrogas, India. About 1 g of HAB was transferred to a 10 mm o.d., medium wall Pyrex tube and evacuated by several freeze−pump−thaw cycles to remove free oxygen. After the sample was evacuated to $\sim 10^{-6}$ Torr, 2 atm of xenon gas was loaded into the sample tube, which was then flame sealed. The sample tube was kept at 350 K (isotropic phase) for 24 h, to enable better dissolution of xenon gas. The ^{129}Xe chemical shifts and T_1 measurements were carried out on a Varian UNITY-400 spectrometer operating at 110.6 MHz. A broadband 10 mm probe with variable temperature capability was employed. A single 90° excitation pulse (pulse width 21 μs) with a 60 s recycle delay was used to obtain the spectra for chemical shift measurements, and by inversion-recovery sequence 300 s recycle delay was used for T_1 measurements. Xenon gas at low pressure served as an external frequency reference and was set to 0 ppm (at 295 K). To ensure uniform orientational order in the magnetic field, the sample was first heated to its isotropic phase and then cooled in 1 or 2 K steps. The temperature was allowed to equilibrate for 30 min prior to each measurement. Chemical shift measurements were repeated several times to average experimental error. The accuracy of the T_1 measurements is estimated to be within 5%. Density measurements were made as a function of temperature using a capillary pycnometer. The details of the experimental setup and procedure can be found elsewhere.[20]

Theoretical Background

In addition to the macroscopic bulk susceptibility effect, the local orientational order and the density of the medium are primarily responsible for chemical shielding of the xenon nucleus.[3] In the pairwise additive model,[17] Ylihautala et al. have considered another significant term that takes into account the interaction between xenon atoms and liquid crystal molecules, through a molecular pair correlation function and its dependence on temperature. The shielding tensor of the solute atom depends on the relative positions and orientations of solute and solvent molecules (pair configuration). The total solute shielding is obtained by summing over all the shielding perturbations induced by the individual solute−solvent pairs. Any change in the pair correlation function that describes the xenon−LC configurations would influence the xenon nuclear shielding. As the changes in the Xe−LC pair configurations are thermally activated, it would be appropriate to consider the temperature dependence for the xenon shielding anisotropy also. When this model is applied to an uniaxial environment such as the nematic phase, the temperature dependence of the xenon shielding tensor element in the direction of the external magnetic field is written as[17]

$$\sigma_{(T)} = \rho_0(1 - \alpha(T - T_0))\left\{\sigma_0[1 - \epsilon(T - T_0)] + \frac{2}{3}\Delta\sigma_0[1 - \Delta\epsilon(T - T_0)]S_{(T)}P_2(\cos\beta)\right\} \quad (1)$$

Here, ρ_0 is the density of the liquid crystal at the reference temperature, α is the thermal expansion coefficient, T_0 is the reference temperature (T_{NI}), and σ_0 and $\Delta\sigma_0$ are the isotropic shielding constant and the shielding anisotropy, respectively, at $T = T_0$ (note: $\sigma_d = \rho_0\sigma_0$ and $\Delta\sigma_d = \rho_0\Delta\sigma_0$ have the units ppm). The isotropic shielding constant σ_0 describes the spherically symmetric part of the distortion, while $\Delta\sigma_0$ describes the deviation of the electron density distribution from spherical symmetry. The factors ϵ and $\Delta\epsilon$ describe the temperature dependence of the isotropic shielding and the shielding anisotropy, respectively. According to the pairwise additive model, ϵ and $\Delta\epsilon$ carry important but indirect information about the changes in the Xe−LC configurational averages and hence in their pair correlations, with respect to the temperature. The factor $P_2(\cos\beta) = {}^1/_2(3\cos^2\beta - 1)$ is the second-order Legendre polynomial, and β is the angle between the director (the molecular direction of the preferred orientation) of the liquid crystal and the direction of magnetic field B_0. The factor $S_{(T)} = \langle P_2(\cos\theta)\rangle$ is the temperature dependence of the second-rank orientational order parameter of the molecular symmetry axis, and θ is the angle between the molecular axis and the director. The angular brackets $\langle\ \rangle$ denote an ensemble average over all values of θ.

According to the well-known McMillan model,[10] the amplitude of the density wave along the z-axis can be described by a mixed translational−orientational order parameter, $\sigma_1 = \langle\cos(2\pi z/d)P_2(\cos\theta)\rangle$, where d is the interlayer spacing. The average value of the translational order parameter of the smectic-A phase is written as $\tau = \langle\cos(2\pi z)/d\rangle$. In the density-modulated phase, the orientational order is position dependent and the positional distribution function of the molecules is

$$\Gamma(z) = \frac{1}{d}[1 + 2\tau\cos(2\pi z/d) + ...] \quad (2)$$

Considering a solute atom such as xenon in the smectic phase, it is expected that its occupancy follows the positional distribution function $\Gamma(z)$ of the LC molecules. Then the translational order parameter of the xenon atoms in the smectic phase can be written as $\tau_{Xe} = \langle\cos(2\pi z/d)\rangle_{Xe}$, which in the simplest case can be approximated as

$$\tau_{Xe} = C\tau \quad (3)$$

where C is a temperature independent constant. According to the phenomenological model[16] the expression for the average nuclear shielding in the smectic phase is given by

$$\sigma_{zz(T)} = \rho_0(1 - \alpha(T - T_0))\left\{\sigma_0[1 + 2\tau_{(T)}\tau_{Xe(T)}] + \frac{2}{3}\Delta\sigma_0[S_{(T)} + 2\sigma_{1(T)}\tau_{Xe(T)}]P_2(\cos\beta)\right\} \quad (4)$$

Substituting τ_{Xe} from eq 3 into eq 4, σ_{zz} can be expressed as

$$\sigma_{zz(T)} = \rho_0(1 - \alpha(T - T_0))\left\{\sigma_0[1 + 2C\tau^2_{(T)}] + \frac{2}{3}\Delta\sigma_0[S_{(T)} + 2C\sigma_{1(T)}\tau_{(T)}]P_2(\cos\beta)\right\} \quad (5)$$

Following the pairwise additive model, we make a simple modification to eq 5 to account for the temperature dependence of the isotropic and anisotropic shielding contributions in the smectic phase also. Thus,

$$\sigma_{zz(T)} = \rho_0(1 - \alpha(T - T_0))\left\{\sigma_0(1 - \epsilon(T - T_0))[1 + 2C\tau^2_{(T)}] + \frac{2}{3}\Delta\sigma_0(1 - \Delta\epsilon(T - T_0))[S_{(T)} + 2C\sigma_{1(T)}\tau_{(T)}]P_2(\cos\beta)\right\} \quad (6)$$

In the absence of more reliable X-ray studies for measuring τ, the ^{129}Xe shielding measurements seem to provide some clues about this parameter. In the absence of a smectic phase, that is, $\tau = 0$ and $\sigma_1 = 0$, the above expression reduces to eq 1 given by Ylihautala et al. for the nematic phase. Numerical estimates of the isotropic and anisotropic parts of the chemical shielding and their temperature dependences can be made by fitting the experimental data to eq 6 in three different steps, as follows: (i) $S = \sigma = \tau = 0$, and $T_0 = T_{NI}$, for the isotropic phase. (ii) Setting $S \neq 0$, $\sigma = \tau = 0$, and $T_0 = T_{NI}$ and fixing σ_0 and ϵ to their values in the isotropic phase at T_{NI}, the data in the nematic phase can be analyzed. (iii) In the smectic phase all the order parameters are relevant, and hence, $S \neq \sigma \neq \tau \neq 0$, and $T_0 = T_{SN}$. In summary, eq 6 can be used to understand the chemical shift data in the isotropic, nematic, and smectic phases by specifying an appropriate reference temperature T_0, density, and order parameters.

To analyze the temperature dependence of the ^{129}Xe chemical shift, the three order parameters and the density of the LC must be known. The temperature dependence of the order parameters can be approximated using the McMillan model[10] for smectic phases. According to this model, the distribution function of LC molecules in the smectic phase is

$$f(\theta,z) = \frac{1}{Z}\left[\frac{V_0}{kT}(S + \alpha_0\sigma_1\cos(2\pi z/d))\right]P_2(\cos\theta) \quad (7)$$

where Z is the normalization function

$$Z = \int_0^d dz \int_0^\pi d\theta \sin\theta \exp\left\{\frac{V_0}{kT}[S + \alpha_0\sigma_1\cos(2\pi z/d)]\right\}P_2(\cos\theta) \quad (8)$$

Here, V_0 is the coupling constant and is related to T/T_{NI} through $T/T_{NI} = kT/0.2202V_0$. Thus, V_0 determines the T_{NI} of the LC and fixes the temperature scale of the model. The factor $\alpha_0 = 2\exp[-(\pi r_0/d)^2]$ is the dimensionless interaction strength of the smectic phase and determines T_{SN}/T_{NI}, r_0 is the length of the rigid core of the molecule, d is the layer spacing, and k is Boltzmann's constant. In the case of HAB, T_{SN}/T_{NI} is 0.953, which corresponds to $\alpha_0 = 0.874$. The order parameters S and σ_1 are calculated by numerically solving the self-consistency relations $S = {}^1/_2\langle 3\cos^2\theta - 1\rangle$ and $\sigma_1 = {}^1/_2\langle(3\cos^2\theta - 1)(\cos(2\pi z/d))\rangle$ using the distribution function (eq 7). The value of τ is obtained from the resulting S and σ_1. Solution of the self-consistency relations for S and σ_1 is somewhat involved, given the fact that they are implicit in both S and σ_1. To start the solution procedure, the particle distribution function is expanded in terms of a power series, retaining as many terms as are mandated by the criterion of accuracy, and integration is carried out numerically to evaluate the order parameters. Starting with trial values of S and σ_1, the equation for S is solved first to obtain a new value of S. Repeated calculation of S is continued in this fashion until a converged value of S is obtained. An optimization procedure based on the Newton−Raphson method was used to speed up the process. A similar procedure is followed for the evaluation of the order parameter σ_1. Repeated calculation of both S and σ_1 is continued in a sequential fashion until convergence is obtained for both S and σ. This procedure of evaluation of the order parameters is repeated for various temperatures in the range of interest, yielding the results shown in Figure 1.

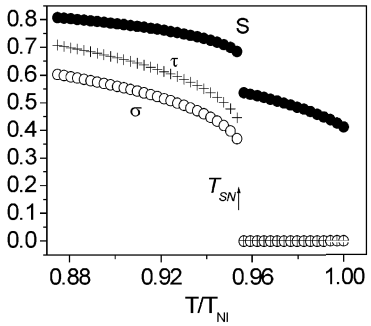

Figure 1. Variation of the theoretically estimated orientational order parameter S, the translational order parameter τ, and the mixed translational−orientational order parameter σ, as a function of reduced temperature T/T_{NI}. These parameters are calculated for $\alpha_0 = 0.874$ (as in the case of HAB), in nematic and smectic phases, using the McMillan model. τ and σ are zero in the nematic phase, as explained in the text.

It is well-known that the variation of the order parameters with temperature can be fitted to Haller's function[21]

$$S_{(T)} \text{ or } \sigma_{1(T)} \text{ or } \tau_{(T)} = (1 - y(T/T_0))^z \quad (9)$$

The order parameters $S_{(T)}$, $\sigma_{1(T)}$, and $\tau_{(T)}$ calculated from the McMillan data (Figure 1) could be satisfactorily fitted to this function. The model parameters y and z thus obtained are given in Table 1.

Substituting ρ_O and α from density measurements and the calculated order parameters $S_{(T)}$, $\sigma_{1(T)}$, and $\tau_{(T)}$ in eq 6, the coefficients σ_0, $\Delta\sigma_0$, ϵ, $\Delta\epsilon$, and C can be evaluated by least-squares fitting to the experimental chemical shift data.

The ^{129}Xe T_1 of xenon atoms dissolved in solvents is mediated mainly through the heteronuclear dipolar interaction between xenon nuclei and protons of hydrogen atoms on the solvent molecules.[22] The predominant dynamic process (with a correlation time τ_c) that modulates the Xe−H dipolar interaction is the translational diffusion of xenon atoms relative to the LC molecules.[23] Assuming an Arrhenius type of temperature

TABLE 1: Fitted Coefficients of the Function $(1 - y(T/T_{NI}))^z$ Describing the Temperature Dependence of the Three Order Parameters, S, σ, and τ, of HAB[a]

	nematic	smectic-A
y of $S_{(T)}$	0.9809 ± 0.0001	1.0312 ± 0.0004
	$(0.9994 \pm 0.0003)^b$	$(1.0432 \pm 0.0003)^b$
z of $S_{(T)}$	0.2235 ± 0.0002	0.0911 ± 0.0003
	$(0.16345 \pm 0.0068)^b$	$(0.0769 \pm 0.0002)^b$
y of $\sigma_{(T)}$		1.0390 ± 0.0002
z of $\sigma_{(T)}$		0.2106 ± 0.0003
y of $\tau_{(T)}$		1.0460 ± 0.0002
z of $\tau_{(T)}$		0.1457 ± 0.0007

[a] The order parameters are calculated using the McMillan model, as described in the text. [b] The values given in parentheses are obtained from the experimentally measured $S_{(T)}$ (^{2}H NMR of HAB) by Catalano et al.[19]

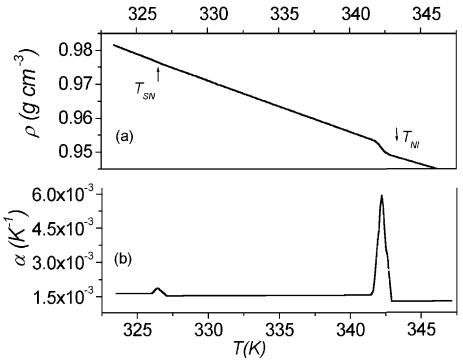

Figure 2. (a) Temperature dependence of the density ρ of the liquid crystal HAB (on decreasing temperature). The arrows indicate the isotropic to nematic and nematic to smectic transition temperatures T_{NI} and T_{SN}, respectively. The density jump across T_{NI} is 0.422%, and that across T_{SN} is about 0.012%. The small change across T_{SN} is not resolved in the plot. (b) Variation of the thermal expansion coefficient, α across the phase transitions from the density studies. α is calculated from the relation $\alpha = (1/V_n)(\Delta V/\Delta T)$, where V_n is the average molar volume for the temperature difference ΔT and where ΔV is the molar volume change across the temperature difference ΔT.

dependence for τ_c ($\tau_c = \tau_0 \exp(E_a/kT)$), the slope $d(\ln T_1)/d(1/T)$ yields the activation energy (E_a) associated with the xenon dynamics. Estimating E_a in different LC phases would allow the determination of potential barriers for xenon dynamics and would give insight into the evolution of the packing environment of LC molecules with temperature. It can be expected that the information obtained from the T_1 measurements would offer a complimentary support to the analysis of xenon chemical shielding data.

Results and Discussion

The temperature dependence of the density of HAB ($\rho_{(T)}$) and the thermal expansion coefficient (α) are shown in Figure 2.

The density varies linearly with temperature in all three phases. The jump in density, $\Delta\rho$, is 0.45% and 0.012% at T_{NI} and T_{SN}, respectively. The thermal expansion coefficient α is calculated from the expression $\alpha = 1/V_n(\Delta V/\Delta T)$, where V_n is the average molar volume and ΔV is the volume change accompanying a change in temperature ΔT. Equilibrium values of α in each phase are taken for the analysis (Figure 2b). The density data can be fitted to linear functions $\rho_{(T)} = \rho_0[1 - \alpha(T - T_0)]$ in the isotropic phase and $\rho_{(T)} = \rho_0[1 - \alpha(T - T_0) + \Delta\rho/\rho_0]$ in the nematic and smectic phases. The values of ρ_0 (g cm^{-3}) and α (K^{-1}) in the isotropic, nematic, and smectic phases are as follows: 0.9494 ($\pm$0.0001) and 13.1×10^{-4} ($\pm 1 \times 10^{-6}$); 0.9494 and 15.9×10^{-4}; 0.9757 and 16.5×10^{-4}, respectively.

After making the bulk susceptibility correction,[24] which is only about 0.6% throughout the temperature range, the temperature dependences of the ^{129}Xe chemical shifts $\sigma_{zz(T)}$ are shown in Figure 3. In the isotropic phase the chemical shift varies linearly with temperature (0.225 ppm K^{-1}). Around 342 K the data exhibit a downfield jump of about 5 ppm corresponding to the I$-$N transition, and the variation of chemical shift in the nematic phase is nonlinear. Upon passing through the transition from the nematic phase to the smectic phase (327 K), the chemical shift has continuously decreased by about 1.2 ppm. The chemical shift within the smectic phase varied slowly with temperature and moved to downfield again near the smectic$-$solid transition (307 K). Spectra were acquired down to 299 K, below which the line broadens beyond its detection.

As discussed above, we have attempted to fit the experimental chemical shift data to the theoretical expression (eq 6). As the number of fitting variables increases in nematic and smectic phases, the reliability of the best fit values depends on the constraints applied. Here, the reliability of the fit could be improved by eliminating ρ_0 and α as fitting variables in eq 6. These two variables were experimentally measured from the density studies carried out in the present work (Figure 2) and were used as constants in eq 6. For similar reasons, we used $S_{(T)}$ values from the ^{2}H NMR studies of HAB reported by Catalano et al.[19] In the case of LC molecules oriented along the magnetic field (z-axis), the largest component of the orientational order is along the z-axis and can be expressed as $S_{zz} = P_2(\cos\beta)(1 - y(T/T_0))^z$. Fitting this expression to the S_{zz} values obtained from ^{2}H NMR studies has yielded $\beta = 16.1° \pm 0.5°$, $y = 0.9994 \pm 0.0003$, and $z = 0.16345 \pm 0.0068$ for the nematic phase and $y = 1.0432 \pm 0.0003$ and $z = 0.076 \pm 0.0025$ for the smectic phase. The values of the coefficients for the nematic phase fall within the expected range for a similar type of liquid crystals.[25,26] However, the marginally high values of y (closer to 1) for HAB indicate that the temperature variation of S close to T_{NI} and T_{SN} is experimentally somewhat stronger than that predicted by mean-field theory. The value of β seems to be reasonable for HAB.

Isotropic Phase. First, the isotropic phase is analyzed by setting $S = \sigma = \tau = 0$ in eq 6. The resultant expression is simple and linear in ρ and ϵ. As ρ_0 and α are known from the density measurements, the only adjustable parameters are σ_0 and ϵ, which are evaluated from a least-squares fit to be -200.9 ± 0.005 (ppm cm^3 g^{-1}) and $(1.00 \pm 0.04) \times 10^{-5}$ (K^{-1}), respectively. The coefficient for the temperature dependence of the isotropic part of the chemical shift, ϵ, is almost 2 orders of magnitude smaller than the thermal expansion coefficient, α (1.31×10^{-3} K^{-1}). This observation suggests that the temperature dependence of chemical shielding in the isotropic phase of HAB is mainly due to the change in the liquid crystal density. This is further confirmed from an estimate of the relative change in shielding per unit temperature in the isotropic phase: $1/\delta(\Delta\delta/\Delta T)$ is about 12.4×10^{-4} K^{-1}, which is equal to the relative change in density of the isotropic phase. Furthermore, the observed ϵ is about 1 order of magnitude smaller than that observed in the other two liquid crystals (EBBA and its binary mixture with ZLI 1167).[17,18] It can be inferred from the above results that, in the isotropic phase of HAB, the shielding perturbations of the xenon cloud do not depend on the xenon$-$LC molecular pair correlation function. The energy of the xenon$-$LC collisions seems to have no significant contribution

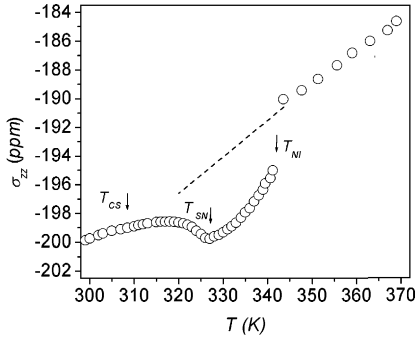

Figure 3. Temperature dependence of the ^{129}Xe chemical shifts of xenon gas dissolved in HAB, after applying bulk susceptibility corrections. The shifts are measured with reference to an external xenon gas sample at low pressure, which is set to 0 ppm. The arrows indicate the phase transitions isotropic to nematic, nematic to smectic-A, and smectic-A to solid, at the temperatures T_{NI}, T_{SN}, and T_{CS}, respectively. The dashed line indicates the variation of the chemical shifts in the nematic and smectic phases due to *density alone*, as explained in the text.

TABLE 2: Values of the Refined and Constrained Parameters in Eq 6, To Fit the Experimental ^{129}Xe Chemical Shielding Data[a]

	isotropic[b]	nematic[b]	smectic-A[c]
ρ_0[d,e] (g cm^{-3})	0.9494	0.9494	0.9757
α[d,e] (K^{-1})	13.1×10^{-4}	15.9×10^{-4}	16.5×10^{-4}
σ_0 (ppm cm^3 g^{-1})	-200.9 ± 0.005	-200.90[e]	-200.90[e]
ϵ (10^{-5} K^{-1})	1.0 ± 0.04	1.0[e]	1.0[e]
$\Delta\sigma_0$ (ppm cm^3 g^{-1})		-13.3 ± 0.3	-12.26[e]
$\Delta\epsilon$ (10^{-4} K^{-1})		-49.1 ± 0.6	-40.0 ± 0.4
y of $S_{(T)}$		0.9994[e]	1.0432[e]
z of $S_{(T)}$		0.1634[e]	0.076[e]
y of $\tau_{(T)}$			1.0442 ± 0.0001
z of $\tau_{(T)}$			0.1454 ± 0.0004
C			-0.0779 ± 0.0012

[a] The refined parameters are obtained by a least-squares fitting method as explained in the text. [b] $T_0 = T_{NI} = \sim 342$ K. [c] $T_0 = T_{SN} = 327$ K. [d] Obtained from density measurements. The product of ρ_0 and σ_0 (or $\Delta\sigma_0$) has the units ppm and yields the isotropic shielding constant and shielding anisotropy at T_0. [e] Fixed during the analysis.

to the isotropic part of the chemical shift in HAB, compared to that in other LCs.

Nematic Phase. The calculated isotropic average shielding is extrapolated to the nematic and smectic phases, and it is linear in these phases (shown as the dotted line in Figure 3), whereas the experimental data are entirely different, with nonlinear behavior. This observation suggests that there could be other contributions stronger than the density effects in these phases. The jump ($\sim$5 ppm) in chemical shielding at T_{NI} to a less shielded value is mainly due to a deviation of the electron cloud from spherical symmetry,[17] resulting in shielding anisotropy. Nevertheless, the contribution due to the increase in the density of HAB at the I−N phase transition is about 0.85 ppm (Figure 3). Choosing $S \neq 0$ and $\sigma = \tau = 0$ in eq 6, the data in the nematic phase are analyzed. Due to the possible pretransitional effects on entering into the smectic phase,[19] five data points between $T/T_{NI} = 0.97$ and 0.958 are omitted from the fitting. The parameters σ_0 and ϵ are kept fixed at the values determined in the isotropic phase with $T_0 = T_{NI}$, and the coefficients y and z for $S_{(T)}$ are constrained to the values given in Table 1. Then the only adjustable parameters left for fitting the nematic data are $\Delta\sigma_0$ and $\Delta\epsilon$, which are refined to values of -13.3 ± 0.3 (ppm cm^3 g^{-1}) and $(-49.0 \pm 0.6) \times 10^{-4}$ (K^{-1}), respectively (Table 2). The fit looks good throughout the range of analysis (Figure 4).

The negative value of $\Delta\sigma_0$ is consistent with the case that the director lies along the direction of B_0.[17,18] As described

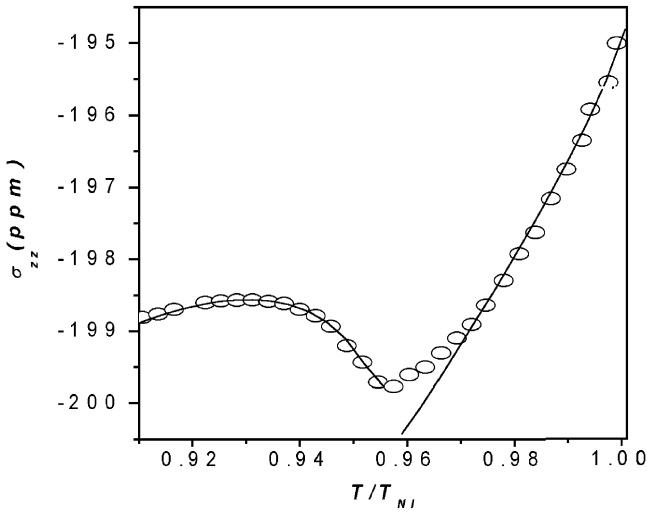

Figure 4. ^{129}Xe chemical shifts as a function of reduced temperature T/T_{NI} in the nematic and smectic phases of HAB. The solid lines are nonlinear least-squares fits to the theoretical expression (eq 6). In the nematic phase σ and τ are set to zero, as required by this case. Because of the pretransitional effects on entering into the smectic phase, experimental data between 326 and 330 K ($T/T_{NI} = 0.955-0.966$) are excluded from the fitting.

already, $\Delta\sigma_d$ or $\rho_0\Delta\sigma_0$ represents the strength of the distortion of the spherically symmetric xenon electron cloud by the anisotropic LC environment and $\Delta\epsilon$ measures its coupling with the temperature. In other words, $\Delta\epsilon$ carries indirectly information about the variations in the positional and orientational configurations of Xe−LC pairs, with respect to the temperature. The larger the magnitude of $\Delta\sigma_d$, the greater is the distortion imposed by the solvent medium. Using phenomenological or pairwise additive models, the $\Delta\sigma_d$ values obtained for the nematic phases of NCB-84,[16] EBBA,[17] and the EBBA−ZLI1167 mixture[18] are much larger in magnitude compared to that obtained for HAB (-12.6 ppm) in the present study. This observation suggests that, in the nematic phase of HAB, the xenon electron cloud be relatively less distorted from its spherical symmetry. The C−H dipolar couplings of methane gas dissolved in EBBA and its binary mixtures showed that EBBA distorts the geometry of the solute atoms to a large extent.[13,27] The observed $\Delta\epsilon$ [$(-49.0 \pm 0.6) \times 10^{-4}$ (K^{-1})] is much larger in magnitude and opposite in sign to α (15.9×10^{-4} K^{-1}), indicating that solute−solvent pair correlations have a significant contribution to the anisotropic shielding. This results in a reduction in the average anisotropy of the local shielding tensor (the anisotropic part of eq 6 without a contribution from the orientational order parameter) with decreasing temperature. For example, on cooling to 327 K, this value decreases from -13.30 to -12.26 (ppm cm^3 g^{-1}). The derived $\Delta\epsilon$ for the nematic phase of HAB is smaller in magnitude compared to that of EBBA (-63.6×10^{-4} K^{-1}), which suggests that the variation in the configurational average of Xe−LC pairs with respect to temperature is relatively weak in HAB.

Smectic-A Phase. In the smectic phase at 327 K ($T/T_{NI} = 0.9575$), the chemical shift decreases to more shielded values by $\sim$1.2 ppm, which suggests that the xenon atoms are experiencing a less anisotropic environment throughout the phase. This is in conformity with similar observations in the other two smectic liquid crystals and can be attributed to the redistribution of xenon atoms into the interlayer spacing of the smectic phase.[15,16] The effect of this intriguing phenomenon on the shielding parameters can be estimated by fitting $\sigma_{(T)}$ to eq 6 with all the order parameters being present. The relevant

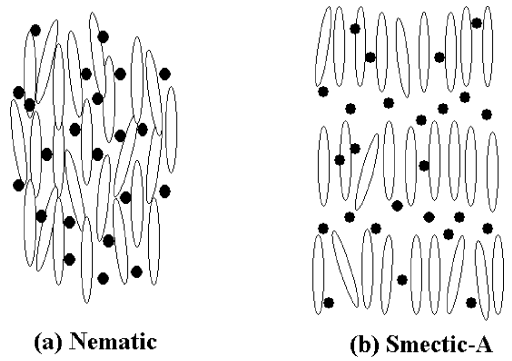

Figure 5. Schematic representation of the occupancy of xenon atoms (●) in the nematic and smectic-A phases in HAB. For the sake of clarity, the molecular arrangement as well as the occupancy of xenon atoms is exaggerated and is not to scale.

coefficients, y and z, of S, σ_1, and τ are given in Table 1. The value of $\Delta\sigma_0$ at $T_0 = 327$ K is calculated from nematic phase data to be -12.26 (ppm cm^3 g^{-1}) (i.e., $\Delta\sigma_d = -11.96$ ppm), which has been kept constant during the fit. The optimized values for a best fit (Figure 4) are $\Delta\epsilon = (-40.1 \pm 0.4) \times 10^{-4}$ K^{-1}, $C = -0.0779$, and z of $\tau = 0.1454$. By physically changing the sample orientation in an electromagnet, the $\Delta\sigma_d$ was measured earlier for the smectic phase of HAB to be about -10.5 ppm,[13] which is lower in magnitude than that obtained in the present analysis. However, this method has some limitations, whereas the present analysis is more reliable, does not require many involved sample rotations, and can be used to study *both* the nematic and smectic phases. The coefficient $\Delta\epsilon$ in the smectic phase [$(-40.1 \pm 0.4) \times 10^{-4}$ K^{-1}] has smaller magnitudes than that in the nematic phase [$(-49.0 \pm 0.6) \times 10^{-4}$ K^{-1}], which indicates that the average anisotropy does not decrease much with the temperature, compared to the case of the nematic phase. It is inferred from the analysis of nematic and smectic phases that the deformation forces in HAB, which cause xenon shielding anisotropy, are relatively weak compared to those observed for other LCs (NCB-84, EBBA, and the EBBA-ZLI1167 mixture). Unfortunately, the comparisons of these findings are limited to only a few LCs due to the unavailability of data from similar modeling studies.

Using eq 3, τ_{Xe} of solute atoms in the middle of the smectic phase (~317 K, $T/T_{NI} = 0.928$) is calculated to be -0.053, which is 7.8% of τ. Following eq 2, this result suggests that the positional distribution function of the xenon atoms,

$$\Gamma_{Xe}(z) = \frac{1}{d}[1 + 2\tau_{Xe}\cos(2\pi z/d) + ...] \qquad (10)$$

decreases in the smectic phase by about 8% from its uniform distribution. The negative sign of τ_{Xe} indicates that the xenon atoms prefer to occupy the interlayer spacing of the smectic phase ($z = d/2$), as they are being expelled from the more dense and oriented aromatic core region ($z = 0$ or d). A schematic representation of this situation is shown in Figure 5.

The deviation of $\Gamma_{Xe}(z)$ is marginally higher in HAB than that observed for the NCB-84 liquid crystal (~5%).[16] Perhaps this could be due to a relatively large d for HAB. To the best of our knowledge, there are no other ^{129}Xe NMR studies available to compare these findings.

Having obtained all the parameters in eq 6, it is interesting to evaluate the temperature dependence of the specific contributions of the effective isotropic deformation (σ_{iso}) and the shielding anisotropy ($\Delta\sigma_{aniso}$) and their dependence on temperature in the nematic and smectic phases of HAB. These individual contributions can be separated from eq 6 and can be expressed as

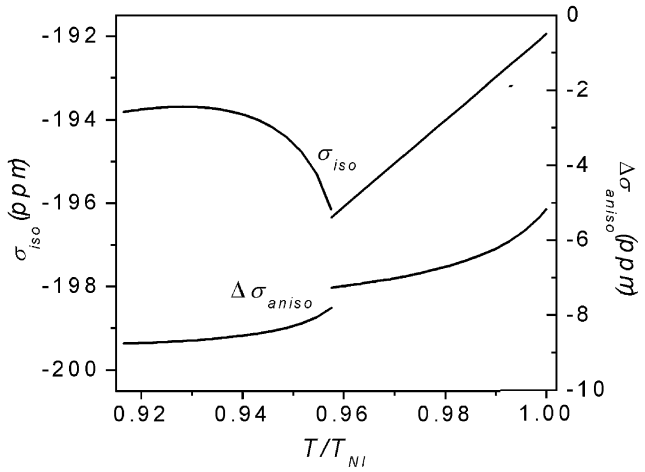

Figure 6. Variation of the isotropic deformational part (σ_{iso}) and the anisotropic shielding part ($\Delta\sigma_{aniso}$) of ^{129}Xe shielding, as a function of reduced temperature (T/T_{NI}) in the nematic and smectic phases of HAB. These contributions are estimated using eqs 11 and 12. The discontinuities around $T/T_{NI} = 0.958$ are due to the N−S transition.

$$\sigma_{iso(T)} = \rho_0(1 - \alpha(T - T_0))[\sigma_0(1 - \epsilon(T - T_0))][1 + 2C\tau^2_{(T)}] \qquad (11)$$

and

$$\Delta\sigma_{aniso(T)} = \rho_0(1 - \alpha(T - T_0))[\Delta\sigma_0(1 - \Delta\epsilon(T - T_0))][S_{(T)} + 2C\sigma_{1(T)}\tau_{(T)}] \qquad (12)$$

and are shown in Figure 6.

The $\sigma_{iso(T)}$ varies linearly in the nematic phase, as expected from eq 11, which is mainly due to the linear variation of density. In the smectic phase, the decrease in the magnitude of $\sigma_{iso(T)}$ can be attributed to a redistribution of xenon atoms toward the interlayer spaces, where the atoms experience a decrease in the solvent density around them. This provides the explanation for the observed reduction in chemical shift ($\sigma_{(T)}$) to more shielded values in this phase.

However, the increase of $\Delta\sigma_{aniso}$ in both nematic and smectic phases is nonlinear, which is due to contributions other than the density of the solvent (Figure 6). On reducing the temperature, $\Delta\sigma_{aniso}$ changes from -5.0 to -7.2 ppm in the nematic phase and from -8.0 to -8.6 ppm in the smectic phase. These variations are much smaller than those observed for other LCs. It may be noted that the earlier measurements based on the sample rotation method could not resolve these details.[13] A detailed examination of $\Delta\sigma_{aniso(T)}$ in these phases suggests that the increase in $\Delta\sigma_{aniso(T)}$ in the nematic phase is essentially due to orientational ordering, $S_{(T)}$, even though the temperature dependence of $\Delta\sigma_0$ (through $\Delta\epsilon$) is significant and opposite to the variation of $S_{(T)}$ (Figure 7).

In the smectic phase also, $S_{(T)}$ makes the major contribution to $\Delta\sigma_{aniso(T)}$. However, in the smectic phase, the temperature dependencies of τ_{Xe} and $\Delta\sigma_0$ are considerable and partially cancel the variation of $S_{(T)}$, thereby resulting in reduction of $\Delta\sigma_{aniso}$ in this phase (Figure 7). This could be the reason for a sluggish variation of $\Delta\sigma_{aniso}$ below $T/T_{NI} = 0.94$. It is important to note that, despite a continuous increase of $\Delta\sigma_{aniso}$ in the smectic phase due to $S_{(T)}$, the ^{129}Xe effective chemical shift

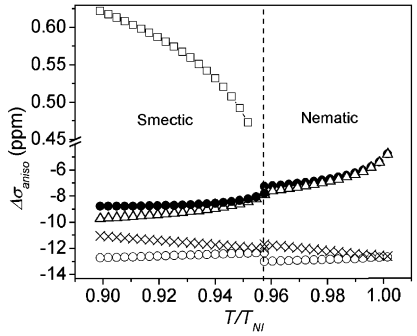

Figure 7. Comparison of the temperature dependence of $\Delta\sigma_{aniso}$ in the nematic and smectic phases as calculated by eq 12 under various conditions: with all parameters being present (●) as shown in Figure 6; with the contribution from $S_{(T)}$ alone (△); with the variation due to $\Delta\sigma_{0(T)}$ alone (×); with the density dependence $\rho_{(T)}$ alone (○), and due to τ_{Xe} alone (□). It can be seen that the total variation is comparable with the variation due to $S_{(T)}$ alone, indicating that increase of $\Delta\sigma_{aniso}$ is mainly due to orientational ordering. In the smectic phase, even though the effective $\Delta\sigma_{aniso}$ has a major contribution from $S_{(T)}$, the other contributions, particularly from τ_{Xe}, scale down the increase of $\Delta\sigma_{aniso}$ with decreasing temperature.

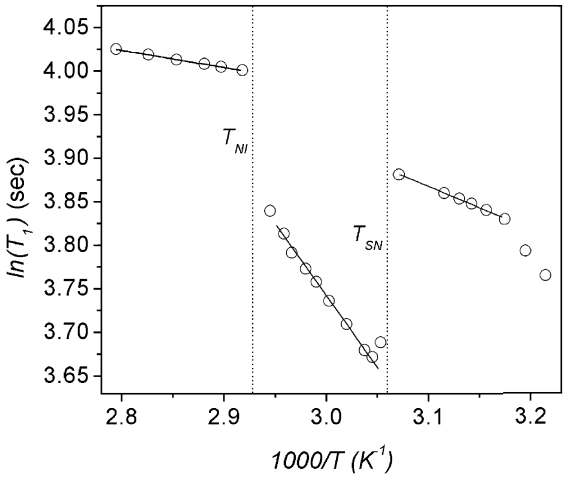

Figure 8. ^{129}Xe ln(T_1) vs 1000/T in HAB, recorded at 9.4 T. Vertical dashed lines indicate the phase transition temperatures. Solid lines are least-squares fits to measure the slopes

($\sigma_{zz(T)}$) decreases because of the reduction in the isotropic deformation contribution σ_{iso}, whose influence is at least 30 times larger than the anisotropic part, that is, $^2/_3P_2(\cos\theta)\Delta\sigma_{aniso}$. Finally, the inference from the above analysis is that HAB seems to be a less deforming medium for xenon atoms compared to the other LCs studied, a feature very crucial in the structural studies of oriented molecules. It would be interesting to extend these studies to mixtures of HAB and the LCs that exhibit smaller dipolar couplings.

Spin−Lattice Relaxation Times. The ^{129}Xe T_1 data exhibit steep variations at isotropic−nematic and nematic−smectic transitions and an increase in slope at the smectic−solid transition (Figure 8), indicating that the relaxation process is very sensitive to the phase transitions. In the isotropic phase, T_1 is about 53 ± 3 s with nominal temperature dependence. Due to the fast diffusion of xenon atoms as well as liquid crystal molecules, the relaxation process is not efficient in this phase. The activation energy measured from the slope in the isotropic phase is 1.64 ± 0.03 kJ mol^{-1}. This value is much lower than that observed for certain binary mixtures.[14] In the uniaxial environment of the nematic phase, liquid crystal molecules can undergo three types of dynamic processes, viz., reorientational motions about their long molecular axis, fluctuations along this axis about their mean positions, and self-diffusion. However, the relative contributions will vary for different liquid crystalline phases. The diffusing xenon atoms "see" an average of all these dynamics processes through a resultant heteronuclear dipolar interaction with protons of the LC, which can be described by a correlation time τ_c. Chemical shift anisotropy (CSA) is the other possible relaxation mechanism. However, it is known from our earlier studies of magnetic field dependent T_1 measurements on other liquid crystals that the CSA contribution is not significant.[14] On cooling the sample, T_1 jumps at T_{NI} to a lower value of 43 s, which could be due to an increase in the molecular packing and order below the isotropic phase.

The observed jump in T_1 then can be attributed to slowing down of the dynamics of LC molecules as well as xenon atoms (increase in τ_c). The higher slope in the nematic phase with a continuos decrease in T_1 values supports this possibility. The activation energy measured from the linear portion of the slope in the nematic phase is 14.0 ± 0.4 kJ mol^{-1}, which is lower compared to that observed in other nematic LCs.[14] A steep increase in T_1 from 28 to 48 s on approaching the smectic phase and its variation within the smectic phase with lesser slope is rather interesting. This behavior suggests that the xenon atoms are diffusing more freely in the low-density regions of interlayer spaces. The activation energy measured from the slope in the smectic phase is 4.0 ± 0.1 kJ mol^{-1}, which is 3.5 times smaller than that in the nematic phase. It is expected that xenon atoms exchange rapidly between layer spacings and interiors, resulting in an average T_1. These observations from xenon dynamics corroborate the analysis of chemical shielding data and also support the possibility of HAB being a relatively less distorting medium.

Conclusions

We have carried out systematic studies to probe the isotropic and anisotropic environments of the HAB liquid crystal using ^{129}Xe chemical shifts and T_1, which showed clear signatures of the phase transitions that HAB exhibits. We have employed the pairwise additive model to account for the temperature dependence of ^{129}Xe chemical shifts and the isotropic (σ_{iso}), and anisotropic ($\Delta\sigma_{aniso}$) parts of the shielding contributions are determined.

The temperature dependence of nuclear shielding in the isotropic phase is exclusively due to the density change alone, and there is no significant role of the xenon−LC pair correlation function in this phase.

In the nematic and smectic phases the $\Delta\sigma_{aniso}$ is mainly due to the orientational order parameter $S_{(T)}$ along with a significant role of the xenon−LC pair correlation function. In the smectic phase, xenon atoms redistribute toward the interlayer spacing with a deviation from the uniform distribution by about 8%.

The ^{129}Xe T_1 in HAB is very sensitive to the phase transitions. These studies have shown that the diffusion of xenon atoms is more constrained in the nematic phase. In the smectic phase, xenon atoms preferentially occupy the interlayer spaces and undergo relatively fast diffusion. These results are in agreement with the conclusions drawn from the analysis of chemical shift data.

Finally, HAB seems to be a less distorting medium for xenon atoms compared to other LCs reported in the literature. Further studies on mixtures of HAB and LCs that exhibit smaller dipolar couplings would be interesting. Such an exercise can help in searching new LC solvents for orienting molecules for NMR structural determinations.

Acknowledgment. This work is financed by IICT under *Prolog to Discovery*. M.H.V.R.R. thanks CSIR, India for financial assistance.

References and Notes

(1) Fraissard, J.; Ito, T. *Zeolites* **1988**, *8*, 350. (b) Raftery, D.; Chmelka, B. F. *NMR basic principle and progress*; Springer-Verlag: 1994; p 30.
(2) Bayel, J. P.; Courtieu, J.; Jullien, J. *J. Chim. Phys*. **1988**, *85*, 147.
(3) Jokisaari, J. *Prog. NMR Spectrosc*. **1994**, *26*, 1.
(4) Bowers, C. R.; Storhaug, V.; Webster, C. E.; Bharatam, J.; Cottone, A.; Gianna, R., III; Betsey, K.; Gaffney, B. J. *J. Am. Chem. Soc*. **1999**, *121*, 9390.
(5) Chmelka, F.; Raftery, D.; McCormick, A. V.; de Menorval, L. C.; Levine, R. D.; Pines, A. *Phys. Rev. Lett.* **1991**, *66*, 580−583.
(6) Bifone, A.; Song, Y. Q.; Seydoux, R. E.; Taylor, B. M.; Goodson, T.; Pietrass, T.; Budinger, T.; Navon, G.; Pines, A. *Proc. Natl. Acad. Sci. U.S.A.* **1996**, *93*, 12932−12936.
(7) (a) Bowers, C. R.; Pietrass, T.; Barash, E.; Pines, A.; Grubb, R. K.; Alivisatos, A. P. *J. Phys. Chem.* **1994**, *98*, 9400−9404. (b) Haake, M.; Pines, A.; Reimer, J. A.; Seydoux, R. *J. Am. Chem. Soc.* **1997**, *119*, 11711−11712.
(8) Sakai, K.; Bilek, A. M.; Oteiza, E.; Walsworth, R. L.; Balamore, D.; Jolesz, F. A.; Albert, M. S. *J. Magn. Reson., Ser. B* **1996**, **1996**, *111*, 300.
(9) Khetrapal C. L.; Kunwar, A. C. *Adv. Magn. Reson*. **1977**, *9*, 302.
(10) McMillan, W. L. *Phys. Rev. A* **1971**, *4*, 1238.
(11) (a) Dong, R. Y. *Nuclear magnetic resonance of liquid crystals*; Springer-Verlag, 1994. (b) Emsley, J. W. Measurement of orientational Order in Liquid Crystalline Samples by NMR Spectroscopy. In *Recent Advances in Liquid Crystalline Polymers*; Chapoy, L., Ed.; Elsevier: 1984; pp 245−251.
(12) Jokisaari, J.; Diehl, P. *Liq. Cryst.* **1990**, *7*, 739.
(13) Muenster, O.; Jokisaari; Diehl, P. *J. Mol. Cryst. Liq. Cryst*. **1991**, *206*, 179.
(14) Bharatam, J.; Bowers, C. R. *J. Phys. Chem. B* **1999**, *103*, 2510.
(15) Ruohonen, J.; Ylihautala, M.; Jokisaari, J. *Mol. Phys.* **2002**, *99*, 711.
(16) Lounila, J.; Muenster, O.; Jokisaari, J. *J. Chem. Phys*. **1992**, *97*, 8977.
(17) Ylihautala, M.; Lounila, J.; Jokisaari, J. *J. Chem. Phys*. **1999**, *110*, 6381.
(18) Ruohonen, J.; Jokisaari, J. *Phys. Chem. Chem. Phys.* **2001**, *3*, 3208 and references cited therein.
(19) Catalano, D.; Forte, C.; Veracini, C. A.; Emsley, J. W.; Shilstone, G. N. *Liq. Cryst.* **1987**, *2*, 345.
(20) Rao, N. V. S.; Pisipati, V. G. K. M. *J. Phys. Chem*. **1983**, *87*, 899.
(21) Haller, I. *Prog. Solid State Chem*. **1975**, *10*, 103.
(22) Moschos; Reisse, J. *J. Magn. Reson.* **1991**, *95*, 603.
(23) Abragam, A. *The Principles of Nuclear Magnetism*; Calrendon Press: Oxford, 1961.
(24) Buckingham, A. D.; Burnell, E. D. *J. Am. Chem. Soc.* **1967**, *89*, 3341.
(25) de Jeu, W. H. *Physical Properties of Liquid Crystalline Materials*; Gordon and Beach: New York, 1980.
(26) Buka, A.; de Jeu, W. H. *J. Phys.* **1982**, *43*, 361.
(27) Hiltunen, Y.; Jokisaari, J.; Pulkkinen, A.; Väänänen, T. *Chem. Phys. Lett*. **1984**, *109*, 509.